

# Comparison of multiple DNA dyes for real-time PCR: effects of dye concentration and sequence composition on DNA amplification and melting temperature

Haukur Gudnason<sup>1</sup>, Martin Dufva<sup>1</sup>, D.D. Bang<sup>2</sup> and Anders Wolff<sup>1,\*</sup>

<sup>1</sup>Department of Micro- and Nanotechnology, Technical University of Denmark, bldg. 345, DK-2800 Lyngby and

<sup>2</sup>Laboratory of Applied Micro-nanotechnology, Department of Poultry, Fish, and Fur Animals, The National Veterinary Institute, Technical University of Denmark, Hangevej 2, DK-8200 Aarhus N, Denmark

Received April 29, 2007; Revised August 15, 2007; Accepted August 16, 2007

## ABSTRACT

The importance of real-time polymerase chain reaction (PCR) has increased steadily in clinical applications over the last decade. Many applications utilize SYBR Green I dye to follow the accumulation of amplicons in real time. SYBR Green I has, however, a number of limitations that include the inhibition of PCR, preferential binding to GC-rich sequences and effects on melting curve analysis. Although a few alternative dyes without some of these limitations have been recently proposed, no large-scale investigation into the properties of intercalating dyes has been performed. In this study, we investigate 15 different intercalating DNA dyes for their inhibitory effects on PCR, effects on DNA melting temperature and possible preferential binding to GC-rich sequences. Our results demonstrated that in contrast to the results of SYBR Green I, two intercalating dyes SYTO-13 and SYTO-82 do not inhibit PCR, show no preferential binding to GC rich sequences and do not influence melting temperature,  $T_m$ , even at high concentrations. In addition, SYTO-82 demonstrated a 50-fold lower detection limit in a dilution series assay. In conclusion, the properties of SYTO-82 and SYTO-13 will simplify the development of multiplex assays and increase the sensitivity of real-time PCR.

## INTRODUCTION

Real-time PCR and melting curve analysis (MCA) are state-of-the-art techniques for quantifying nucleic acids,

for mutation detection, and for genotyping analysis. Utilization of real-time PCR continues to expand and many different systems have been developed, including probe-based methods, such as Taqman Probes [1], molecular beacons [2], Sunrise primers [3], Scorpion primers [4] and Light-up probes [5]. An alternative to probe-based methods is the use of DNA intercalating dyes that bind to double-stranded DNA. Usable dyes have much higher fluorescence when bound to double-stranded DNA compared to the unbound state. Indication of specific amplification is subsequently obtained by analysis of the melting curve of the PCR amplicons. Ethidium bromide was used in an earlier description of real-time PCR [6,7]. Later, SYBR Green I became the most widely used DNA dye for real-time PCR applications because of cost efficiency, generic detection of amplified DNA, and its ability to differentiate PCR products by melting curve analysis [8,9]. SYBR Green I has been applied in post real-time PCR melting curve analysis for rapid detection of various organisms, including *Vibrio vulnificus* [10], *Leptonema illini* [11] and *Plum pox virus* [12], for mutations in the human K-ras gene [13] and for measurement of cell number in microtitre plate cultures [14]. SYBR Green I remains widely used despite numerous studies demonstrating its disadvantages such as extensive optimization [15,16], inhibition of PCR in a concentration-dependent manner [9,17], effects on DNA melting temperature [9,18], and preferential binding to certain DNA sequences [18]. The drawback of using SYBR Green I for melting curve analysis is that the melting temperature is highly dependent on the dye concentration [9] and the DNA concentration [19]. These drawbacks limit the use of SYBR Green I for resolving multiplex PCR based on MCA [18].

Only a limited number of alternative dyes such as BEBO [20], YO-PRO-1 [21], LC Green [22], and SYTO-9

\*To whom correspondence should be addressed. Tel: +45 45256305; Fax: +45 45887762; Email: aw@mic.dtu.dk

[23,24] have been evaluated for use in real-time PCR. In this study, we report a screen of fifteen intercalating dyes for use in real-time PCR and melting curve analysis that span a wide range of dye families and optical properties.

## MATERIALS AND METHODS

### DNA purification

Chromosomal DNA from *Campylobacter jejuni* (*C. jejuni*) type strain CCUG-11284 was isolated using a method described by Machiels *et al.* [25] with modifications [26]. The DNA was eluted in 100  $\mu$ l of pre-heated [65°C] sterile water. DNA concentrations were determined at OD 260 nm using a spectrophotometer (Ultrospec 2000, Pharmacia Biotech, Cambridge, UK). The DNA preparations were stored at -20°C before use.

### Primers and PCR conditions

The primer sequences and the PCR conditions used in this study are summarized in Table 1 and were previously described [27]. The length of the PCR amplicons and the GC content were obtained from the NCBI Genbank database. Two primer sets, UB-FW/UB-RW and UC-FW/UC-RW were used to amplify 300 bp (51.5%GC) and 144 bp (54.9%GC) fragments of the 16S rRNA gene, respectively. A third primer set HIP-FW/and HIP-RW, was used to amplify a 149 bp (37.3%GC) fragment from the *hippuricase* gene of *C. jejuni*.

All PCR mixtures (20  $\mu$ l) contained final concentrations of 200  $\mu$ M of each deoxynucleotide triphosphate (Sigma-Aldrich, Brøndby, Denmark), 1 $\times$  PCR buffer (Applied Biosystems, Foster City, CA, USA), 2.5 mM MgCl<sub>2</sub> (Applied Biosystems), 0.05 U/ $\mu$ l AmpliTaq Gold DNA polymerase (Applied Biosystems), 0.5  $\mu$ M of each primer (Sigma-Aldrich) and 2 ng of *C. jejuni* DNA (10<sup>5</sup> copies). The thermocycling consisted of an initial incubation at 94°C for 4 min followed by 50 cycles of 94°C for 30 s, 60°C for 30 s and 72°C for 30 s and a final extension step of 10 min at 72°C. Multiplex PCRs were performed in the same manner using 0.5  $\mu$ M of each primer with two or more primer pairs.

### Real-time PCR and melting curve analysis

All real-time reactions were performed on a DNA engine thermocycler equipped with a Chromo4 real-time detector

(Bio-Rad Laboratories Inc., Hercules, CA, USA) using thin-walled 100  $\mu$ l white PCR tube strips (Abgene, Surrey, UK). The concentrations of the dyes (Invitrogen, CA, USA) used in this study ranged from 0.1 to 20  $\mu$ M. The molecular concentration of SYBR Green I was calculated using the value from Zipper *et al.* [28]. It was estimated that a 1 $\times$  SYBR Green I solution was equivalent to 2  $\mu$ M. The concentration of the other dyes was calculated based on the concentration of the stock solution given by the supplier. Fluorescent measurements were acquired for all four spectral channels (Table S1 in Supplementary Data) at the end of each 72°C extension step. Melting curves were acquired for PCR products generated during real-time PCR amplification reaction or by conventional PCR without the presence of any dyes. In the latter case, the dyes were added after PCR and melting curves subsequently measured in the real-time PCR thermocycler. Fluorescence signals during the melting of the PCR products were monitored in all four spectral channels using 0.5°C steps with a hold of 10 s at each step from 60°C to 98°C. The differentiated melting curve data analysis was done using the Opticon Monitor version 2.03.5 software (Bio-Rad Laboratories Inc., Hercules, CA, USA) to identify each peak and to extract raw data for further analysis. Detailed data processing and analysis was performed using Origin version 7 (Origin-Lab, MA, USA) with the peak analysis add-on to extract peak height and area. In some cases, the samples were further analyzed by capillary gel electrophoresis (CGE) (Agilent 2100 Bioanalyzer, CA, USA) using the DNA1000 chip set and following the protocol given by the supplier.

## RESULTS

We investigated the inhibitory effect, the effect on DNA melting temperature, and the preferential binding to a certain PCR product in a multiplex PCR system for 15 different intercalating dyes. Of the 15 intercalating dyes tested, PO-PRO-3 was the only DNA dye that did not give a detectable fluorescent signal in the presence of double-stranded DNA and was therefore excluded from any further experiments.

### Inhibition effect of DNA dyes on real-time PCR

The inhibition effects of the respective dyes were investigated using real-time PCR where the concentration

**Table 1.** Primer sequences of the three PCR products used in the study and the corresponding PCR product length as obtained from the NCBI database

Primer	Sequence	PCR amplicon [NC_003912]	GC content%	T <sub>m</sub> calculated by nearest neighbour [°C]
UB-FW	5'-GCTAA CTCCTG CCAGCAG CCGCGG-3'	307 bp	51	85
UB-RW	5'-GGGCG TGGACTA CCAGGG TATC-3'			
UC-FW	5'-CCGC AACGAGC GCAACC CACG-3'	144 bp	55	84
UC-RW	5'-CATT GTAGC ACGTGT GTC-3'			
HIP-FW	5'-GTACT GCAAAA TTAGT GGCG-3'	148 bp	35	78
HIP-RW	5'-GCAAAA GGCAAA GCATC CATA-3'			

The T<sub>m</sub> was calculated using the online tool from Northwestern University (<http://www.basic.northwestern.edu/biotools/oligocalc.html>).

of input DNA was held constant while the dye concentration was varied for each of the fourteen dyes tested. The  $C_t$  value was used as an indicator of inhibitory effects on PCR efficiency, since significant decreases in efficiency would result in increased  $C_t$  values. The  $C_t$  value was obtained for different concentrations of all of the dyes using PCR with HIP, UB and UC primer sets. The  $C_t$  values were plotted against the dye concentrations for each dye and PCR amplicons used. A linear relationship was observed (Figure 1 and Supplementary Data Figure S1) where the slope of the line indicates the degree of inhibition. The dyes could be divided into four classes according to the degree of inhibition (Table 2).

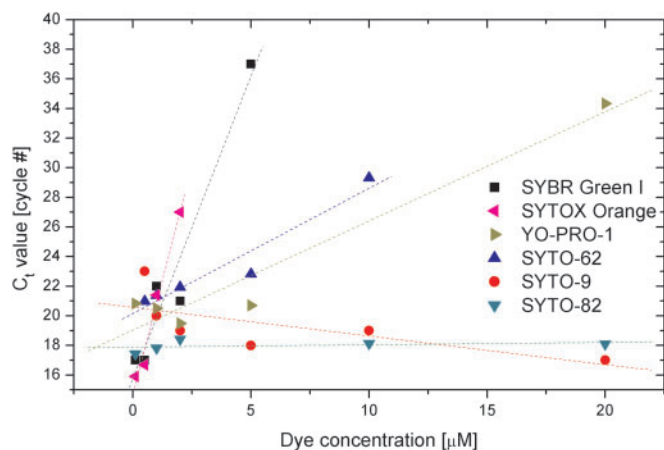


**Figure 1.** Comparison of the threshold cycle ( $C_t$ ) value obtained for six example dyes using the UB PCR to demonstrate the different characteristics of the dyes. The PCR inhibition factor was defined as the average slope for all three PCR products. (See also Supplementary Figure S1)

SYTO-9, SYTO-13, SYTO-16, SYTO-64 and SYTO-82 had very small slope values indicating that the dye had no effect on PCR efficiency even at high concentrations. YO-PRO-1, SYTO-60 and SYTO-62 showed a small increase in  $C_t$  values with increasing concentration of the respective dye indicating that these dyes had a medium inhibitory effect. In contrast, SYTOX Orange, SYBR Green I and TO-PRO-3 showed a large increase in their  $C_t$  values with increased dye concentration indicating that these dyes inhibited PCR to a greater extent at high concentrations. However, even at the recommended concentration for SYBR Green I of  $2\mu\text{M}$  ( $1\times$ ), SYTOX Orange, SYBR Green I and TO-PRO-3 had a negative impact on the  $C_t$  value. The TOTO dye family, TOTO-3, POPO-3 and BOBO-3 showed the largest negative effect on PCR because no  $C_t$  could be determined using these dyes at any concentration. The TOTO dye family is therefore not suitable to use in real-time PCR.

In addition, the effects of dye concentration on PCR of the respective dyes were confirmed by quantification of PCR products after 45 cycles using capillary electrophoresis. All dyes with low inhibition effects (SYTO-9, SYTO-13, SYTO-16, SYTO-64 and SYTO-82) demonstrated no changes in PCR product concentration independent of the dye concentrations, while all the dyes with medium inhibition (YO-PRO-1, SYTO-60, and SYTO-62) showed a slight decrease in PCR product concentration with increasing dye concentration. For high (SYTOX Orange, SYBR Green I and TO-PRO-3) and total inhibition (TOTO-3, POPO-3 and BOBO-3) dyes it was possible to obtain a significant amount of PCR product at very low dye concentrations ( $0.1\text{--}0.5\mu\text{M}$ ). However, the amount of PCR product decreased rapidly with increased dye concentrations and no PCR product was detected at high concentrations ( $5\text{--}20\mu\text{M}$ ).

**Table 2.** Summary of the results obtained for all of the dyes used in this study

	Filter settings	Optimum conc. [ $\mu\text{M}$ ]	maximum $T_m$ shift [ $^{\circ}\text{C}$ ]*	PCR inhibition factor*	Preferential binding*	Fluorescence remaining after thermocycling %	Price per reaction [cent]
SYBR Green I	1	2	$10.3 \pm 0.02$	High	High	74	0.08
SYTO-9	1	2	$1.8 \pm 0.1$	Low	Low	62	1.34
SYTO-13	1	2–5	$0.8 \pm 0.01$	Low	Low	96	0.54
SYTO-16	1	2–5	$2.1 \pm 1.8$	Low	Med	92	2.69
SYTO-60	4	2–5	$5.8 \pm 0.4$	Med	Med	99	0.54
SYTO-62	4	5	$3.3 \pm 0.6$	Med	High	97	0.54
SYTO-64	3	5	$0.7 \pm 0.1$	Low	Low	75	1.34
SYTO-82	2	2	$0.4 \pm 0.03$	Low	Low	90	0.54
POPO-3	2	–	$0.8 \pm 0.8$	Total	Med	62	7.04
TOTO-3	4	–	$1.9 \pm 2.1$	Total	High	92	7.78
BOBO-3	3	–	$2.2 \pm 2.6$	Total	Low	73	6.76
(PO-PRO-3)	2	–	–	–	–	–	0.87
TO-PRO-3	4	2–5	$4.3 \pm 2$	High	Low	86	0.87
YO-PRO-1	1	2–5	$5.80 \pm 0.01$	Med	Med	99	0.84
SYTOX Orange	2	2	$10.0 \pm 0.8$	High	High	90	0.54

The values were determined by using data from all three PCR products, and where applicable, are presented as averages (marked by an asterisk). The maximum  $T_m$  shift represents the average melting temperature difference between low and high dye concentrations. The PCR inhibition factor was defined as the average slope calculated from a  $C_t$  value versus dye concentration graph. The preferential binding is given only as a category classification based on two different multiplex PCR systems. Thermostability represents the fraction of fluorescent signal remaining when measured at  $30^{\circ}\text{C}$  with a fixed amount of DNA after 50 thermal cycles compared to before. This was done in order to evaluate the thermostability of each dye. The prices are calculated assuming a  $20\mu\text{l}$  reaction volume with  $2\mu\text{M}$  dye concentration.

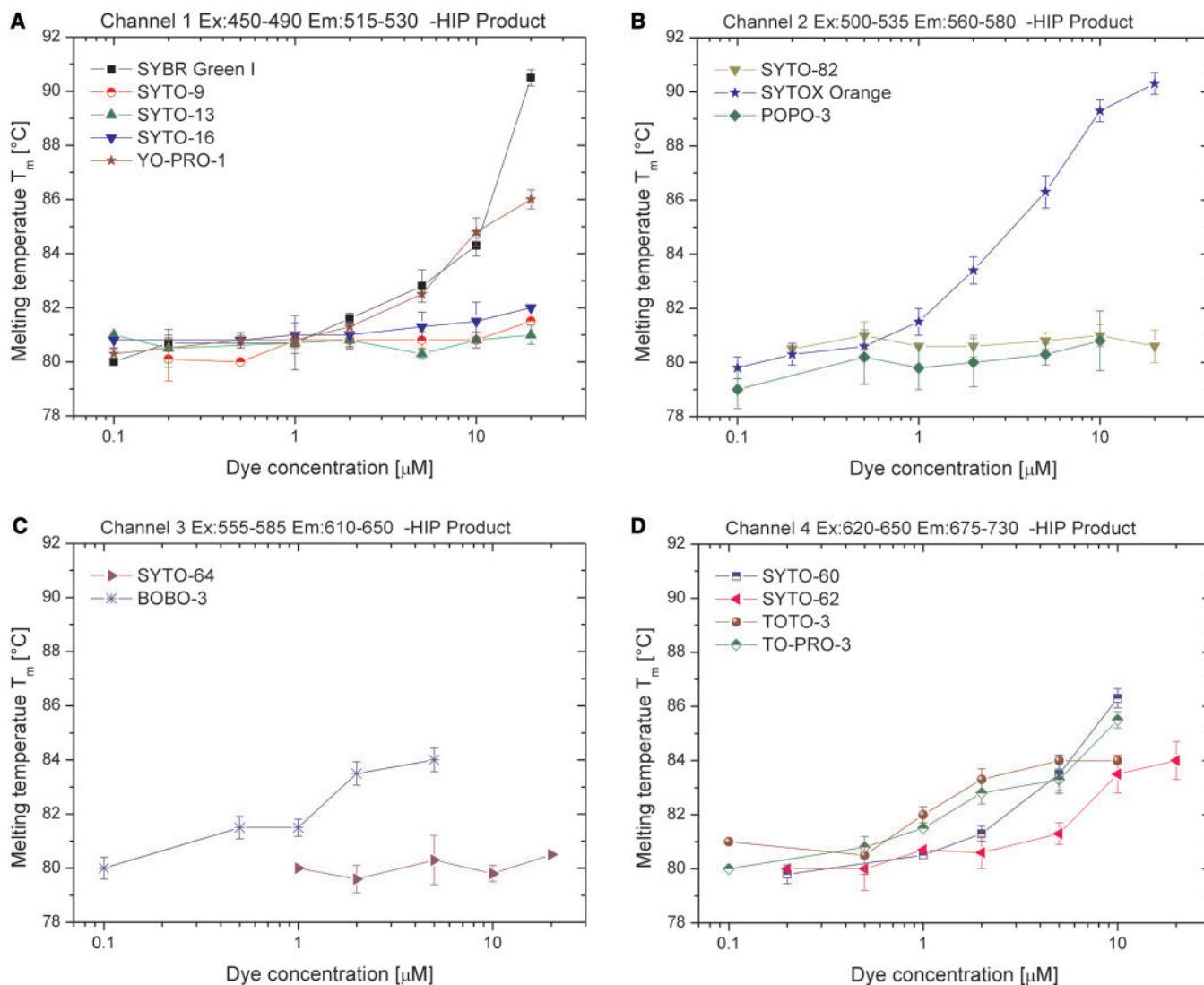


**Figure 2.** Comparison of dye concentration versus  $T_m$  of the HIP amplicon for all four optical channels (A, B, C and D).

### Effect of dye concentration on DNA melting temperature

Intercalating dyes such as SYBR Green I [18,23], EtBr [17], BEBO [20] and TOTO-1 [22] have all been shown to affect the DNA melting temperature of PCR products, which complicates analyses of multiplex reactions. The effect of dye concentration on melting temperature for all 14 dyes was therefore determined. The PCR amplification was performed in the absence of any dye while the concentration of amplified PCR product (10 ng/ $\mu\text{l}$ ) and the  $\text{MgCl}_2$  concentration (2.5 mM) were kept equal in all experiments. Dyes with final concentrations ranging from 0.1 to 20  $\mu\text{M}$  were added post-PCR and the melting curves measured. Distinct melting peaks were obtained for all dyes demonstrating that the dyes are specific for double-stranded DNA. SYBR Green I, SYTO-9, SYTO-16, SYTO-60, SYTO-62, YO-PRO-1, SYTOX Orange, BOBO-3, TOTO-3 and TO-PRO-3 showed an increase in measured  $T_m$  with increasing dye concentration (Figure 2). For example, both SYBR Green I and

SYTOX Orange showed a  $T_m$  increase of roughly  $10^{\circ}\text{C}$  for all three PCR amplicons when 10–20  $\mu\text{M}$  of dyes were used. In contrast, SYTO-82, SYTO-64, SYTO-13, POPO-3 showed no significant increase in measured  $T_m$  throughout the dye concentration range (Table 2). It should be noted that a melting temperature of  $81^{\circ}\text{C} \pm 1^{\circ}\text{C}$  for the HIP PCR amplicon was determined when using 1  $\mu\text{M}$  or lower of any dye tested (Figure 2) while the melting temperatures for UB and UC fragments at dye concentrations of 1  $\mu\text{M}$  or lower was  $87^{\circ}\text{C} \pm 1^{\circ}\text{C}$  (Supplementary Data Figure S2).

### Preferential binding effect of DNA dyes in multiplex real-time PCR

DNA melting temperature analysis can be used to determine the ratio of two or more PCR products in a multiplex real-time PCR. However, Giglio *et al.* [18] showed the preferential binding of SYBR Green I to GC-rich sequences resulting in the detection of only one

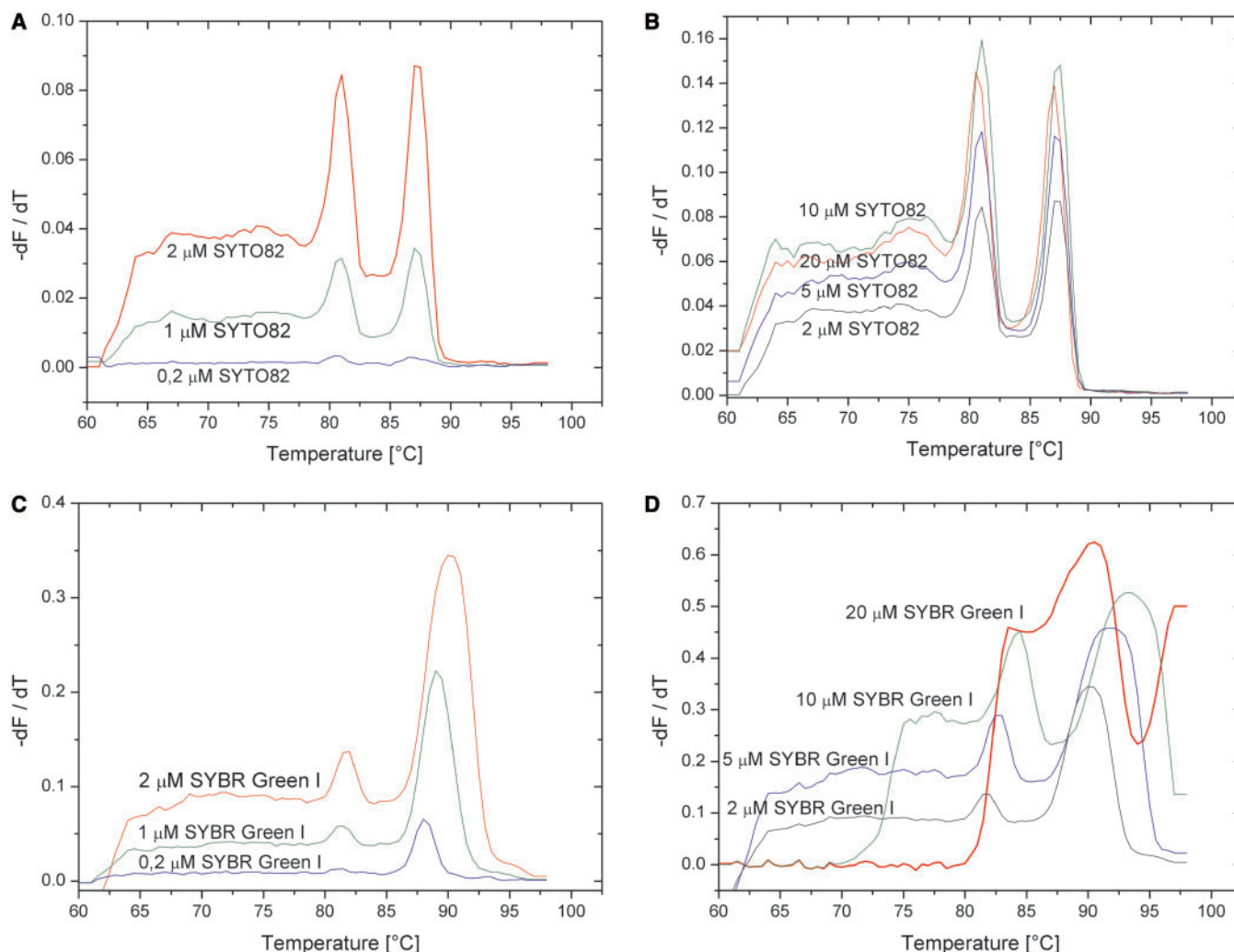


**Figure 3.** Example of multiplex melting curve separation of two products with different concentrations of SYTO-82 (A and B) and SYBR Green I (C and D). The melting curves were for the pre-amplified multiplex PCR with both UC (144 bp, GC 51%, right peak) and HIP (149 bp, GC 37%, left peak) primers. The height of the peak was calculated as the peak height from a baseline defined by the background and the height peak ratio is the ratio of the right peak divided by the left.

amplicon in a multiplex PCR where two amplicons were present as determined by gel electrophoresis. To identify any such preferential binding to amplicons, the effect of dye concentration on the identification of two PCR products by melting curve analysis was investigated. Two multiplex PCR reactions were used, one with UB and HIP products and the other with UC and HIP products. The difference between the two mixtures is that the former has a different length and almost the same GC% content. The latter has the same fragment length but different GC% content, making the fragments indistinguishable in standard gel electrophoreses (data not shown). All PCR fragments were amplified separately and mixed at a ratio of 1:1 at a concentration of 10 ng/ $\mu$ l. The respective dye was added at different concentrations and melting curve analyses were performed to obtain the melting curve peaks for both the HIP product (left peak with  $T_m$  of 80°C) and the UC or UB products (right peak with  $T_m$  of 86°C). Figure 3 shows melting curve examples

for the HIP/UC mixture using SYBR Green I and SYTO-82. The two dyes demonstrate substantially different characteristics. At high dye concentrations of SYBR Green I, both amplicons can be detected with similar heights but the peaks are broad and difficult to analyse (Figure 3D), while at lower dye concentration the peaks become sharper but the HIP peak becomes more difficult to detect (Figure 3C). The best resolution obtained was at a dye concentration of SYBR Green I melting curve analysis). These effects on peak heights and widths were also pronounced for SYTOX Orange, SYTO-62 and YO-PRO-1. In contrast, SYTO-82 showed very little change in the shape of the peaks across the entire concentration range aside from a lower signal intensity attributed to the reduced number of available dye molecules (Figure 3A and B).

To evaluate preferential binding of the dyes to respective fragments, the peak height ratio was plotted

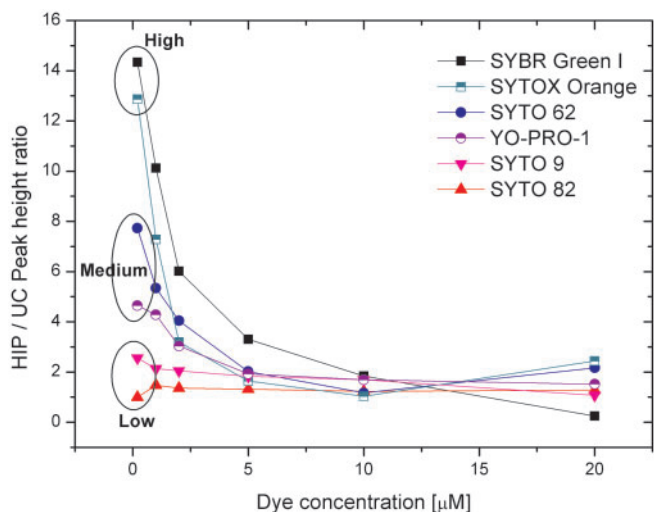


**Figure 4.** Comparison of dye concentration versus the peak height ratio for a few selected dyes in the UC/HIP multiplex PCR reactions (For other dyes see also Supplementary Data Figure S3). The degree of preferential binding for the dyes (low, medium, or high) is indicated in the figure.

against the dye concentration for both the HIP/UC and the HIP/UB fragment mixtures (Figure 4 and Supplementary Figure S3). All of the dyes reach a plateau of the peak ratio between 1 and 2 after the dye concentration reaches 5  $\mu\text{M}$  for both HIP/UC and the HIP/UB fragment mixtures. Below that concentration the dyes behave very differently with some exhibiting very high ratio values while others have no change. For instance, at 2  $\mu\text{M}$  of SYBR Green I, the HIP/UC ratio was determined to be 6 and the HIP/UB ratio was 8 where a ratio of 1 and 2 was expected based on fragment size. In contrast, at 2  $\mu\text{M}$  of SYTO-82, the ratio observed was near 1 for HIP/UC and 2 for HIP/UB fragment mixtures. This shows that the SYBR Green I dye clearly prefers binding to the GC-rich UC and UB products regardless of fragment size. For convenience the dyes have been divided into 3 groups (as indicated in Figure 4), based on the peak ratio data: high, medium and low preferential binding (Table 2).

#### Detection limit of SYTO-82 in real-time PCR compared to SYBR Green I

Detection limits of SYTO-82 in real-time PCR was compared to SYBR Green I by real-time PCR with a DNA template dilution series ranging from 50 to  $10^6$  copies and using 2  $\mu\text{M}$  dye. The detection limit of endpoint PCR as determined by melting curve analysis and confirmed by capillary electrophoresis (Supplementary Data Figure S4) showed that SYBR Green I had a detection limit of 5000 copies of *C. jejuni* DNA while the detection limit using SYTO-82 was 100 copies (Figure 5). In real-time PCR using 2 ng ( $10^5$  copies) DNA template, the use of SYTO-82, showed a 4-fold higher PCR product yield and a  $C_t$  value with four fewer cycles than the same reaction using SYBR Green I. In addition, the detection limit experiment was also performed using a

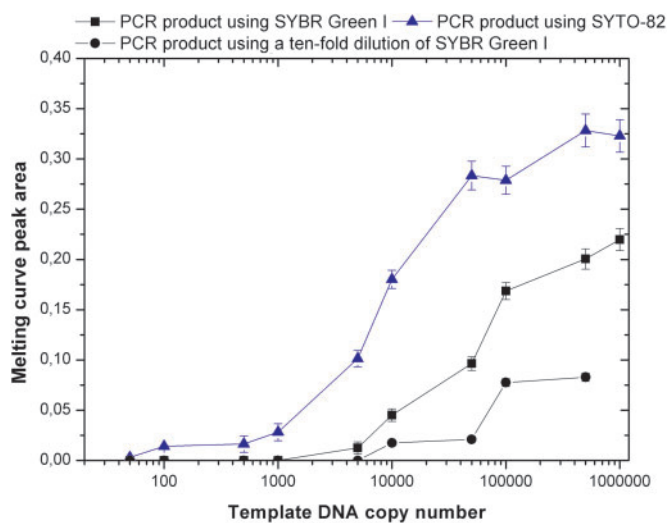


**Figure 5.** The real-time PCR detection limit when using SYBR Green I and SYTO-82 was evaluated by the melting curve peak area. The HIP PCR was performed with a large gradient of template DNA ranging from  $10^6$  to 50 copies of the *C. jejuni* DNA. For SYBR Green I the PCR product melting peak area was measured for both the dye concentrations of 2 and 0.2  $\mu\text{M}$ .

10-times lower concentration of SYBR Green I (0.2  $\mu\text{M}$ ) in order to minimize the PCR inhibitory effect of SYBR Green I. However, no improvement in the detection limit was observed (Figure 5) but more endpoint PCR product was generated (Supplementary Data Figure S4). One common problem often faced in real-time PCR is the formation of primer-dimers and it was observed that SYBR Green I gave three times higher primer-dimer concentrations at low template concentrations in comparison to SYTO-82, and this is probably caused by the DNA stabilizing effect of SYBR Green I.

#### Dye thermostability

The thermostability of all the dyes was investigated by measuring fluorescence with a known amount of DNA at 30°C before and after thermocycling for 50 cycles. Table 2 shows the remaining fluorescent signal (in percentage) for all the dyes after thermocycling. Fluorescent signals were also measured at 72°C during the thermocycling to evaluate the temperature dependence of the dyes because this is the working temperature during real-time PCR. It is known that the fluorescent signal is highly dependent on the temperature [29]. The decrease in fluorescent signal was different for the dyes ranging from only 0.5%/°C to over 1.9%/°C.

A number of the DNA dyes demonstrate fluorescent self-quenching. The dyes SYTO-60, SYTO-62, SYTO-64, POPO-3, TOTO-3, BOBO-3, TO-PRO-3 and SYTOX Orange all demonstrate a clear dependence of fluorescent intensity on the dye concentration with a maximum signal at concentrations situated between 2 and 5  $\mu\text{M}$ . This self-quenching of fluorescent dyes is usually

attributed to increased energy transfer by dye molecule collisions [30].

## DISCUSSION

We have investigated a panel of fluorescent dyes for use in real-time quantitative PCR. The dye SYTO-82 performed better than any of the other dyes tested. It did not preferentially bind to GC- or AT-rich sequences, did not inhibit PCR significantly and demonstrated a 50-fold lower detection limit in a real-time PCR assay compared to SYBR Green I. In contrast, SYBR Green I showed preferential binding to GC-rich sequences, a phenomena previously demonstrated by Giglio *et al.* [18]. At a concentration of 2  $\mu$ M, SYBR Green I inhibited each PCR cycle by about 22% while at a concentration of 20  $\mu$ M SYBR Green I completely inhibited PCR. Such dose-dependent inhibition was not observed for SYTO-82. The decreased detection limit in real-time PCR with SYTO-82 compared to SYBR Green I can be explained by the higher PCR inhibition of SYBR Green I.

The melting temperature of the PCR products was always at least 2°C over the calculated melting temperature. The systematic overestimation of the measured melting temperature may be caused by the dyes binding to the DNA. With the exception of SYTO-13, SYTO-64 and SYTO-82, all other dyes showed a significant increase of melting temperature of the DNA hybrid with increasing dye concentration. This suggests that there is a common stabilizing effect of the dyes on the DNA double helix. The effect was mostly observed at dye concentrations above 2  $\mu$ M. For instance, SYBR Green I, SYTOX Orange and YO-PRO-1 increased the measured  $T_m$  between 6° and 10°C at a 20  $\mu$ M dye concentration. A study performed by Monis *et al.* [23] that compares SYBR Green I and SYTO-9 in a similar manner, revealed a  $T_m$  difference of 10°C for 20  $\mu$ M SYBR Green I. This result is in agreement with our results. There could also be a machine-dependent cause for melting curve temperature differences as suggested by Herrman *et al.* [31]. This difference in melting curves of real-time PCR using SYBR Green I was reported to be in the order of 0.5°C between instruments. This difference is however, negligible when compared with the effect of high concentration of dyes (10°C). The melting temperature shift phenomenon correlates very closely to the measured inhibition effect when both the inhibition, as represented by the  $C_t$  value slope, and  $T_m$  shift are compared together as an average for all three PCR amplicons. The dyes demonstrate a linear correlation suggesting a close relationship between the inhibition of PCR and  $T_m$  shift (Supplementary Data Figure S5). This indicates that the tightness of the dye binding could influence the annealing of the primers or possibly alter the ability of the polymerase to function optimally. This correlation should make it possible to predict, based on the  $T_m$  shift alone, how significant the inhibition effect is for a specific intercalating dye. The PCR inhibition caused by the dyes has a negative effect on the sensitivity of any given assay as could be seen in the comparison between SYBR Green I and SYTO-82, and therefore the use of SYTO-82 could

enhance existing real-time detection assays by increasing PCR efficiency.

The preferential binding of SYBR Green I to specific DNA fragments containing higher GC% content and larger sizes in multiplex PCR with low dye concentrations was demonstrated by Giglio *et al.* [18]. We confirmed this phenomenon for SYBR Green I and other dyes. The preferential binding of the dyes, as measured by the peak ratio, was similarly compared against the  $T_m$  shift demonstrating a linear relationship between the preferential binding of the dye and the  $T_m$  shift. (Supplementary Data Figure S6) This suggests a close connection between the DNA affinity of the dyes and the three properties: amplification inhibition,  $T_m$  shift and preferential binding.

Information from the literature [32–35] and from the manufacturer indicates that inhibition of amplification,  $T_m$  shift and preferential binding can be explained by the affinity of the dye to dsDNA. According to US patent US 5658751, the structure of SYBR Green I is based on a monomeric unsymmetrical cyanine dye [28] with high DNA binding affinity. The TOTO dyes are symmetric dimeric nucleic acid stains that are among the most sensitive and highest affinity fluorescent dyes available for nucleic acid staining while its relative, the TO-PRO family, are smaller monomeric asymmetric cyanine dyes with lower DNA affinity. SYTOX Orange is classified as a SYTO dye but according to Molecular Probes (Invitrogen, CA, USA) it is a high affinity nucleic acid dye. The SYTO dyes are cell permeable cyanine dyes with a relatively low-affinity for nucleic acids [32]. Comparison of the overall performance of the dye families to their reported DNA affinity suggests that DNA affinity is a defining factor for the performance of the dyes as high affinity dyes inhibits PCR to a higher degree compared to low affinity dyes. This can be seen with low affinity SYTO dyes that have the best overall performance while high affinity dyes such as SYBR Green I and SYTOX Orange have very poor performance. In addition, the very high affinity TOTO dyes demonstrate complete PCR inhibition, suggesting that this dye family may interfere with the performance of the polymerase or even primer binding. These results confirm that the tightness of the binding of the dye to DNA influences the measured  $T_m$ , PCR product preference and PCR inhibition.

Following an extensive screening of fluorescent intercalating DNA dyes we have concluded that there are a number of dyes suitable for real-time PCR. Among the 14 dyes tested, most notable are the dyes SYTO-13 and SYTO-82 which performed superbly on all aspects tested such as having a minimal inhibitory effect on PCR, minimal preferential binding and minimal melting temperature shift. The cost difference between SYTO-82 and SYBR Green I is about 7-fold. However, the cost of the dye is not an important factor when compared to the overall cost of the PCR reaction. In our case, the cost of Ampliqaq Gold is about 93 cents (US)/reaction and that corresponds to a dye cost of 0.1% of the total reagent cost for SYBR Green I and 0.6% for SYTO-82. Furthermore, the detection limit using SYTO-82 in a real-time PCR application was 50-fold better than SYBR Green I that easily compensates for the slightly higher cost of

SYTO-82. In conclusion, our results strongly suggest that SYTO-13 and SYTO-82 should replace SYBR Green I in real-time PCR applications.

## SUPPLEMENTARY DATA

Supplementary Data are available at NAR Online.

## ACKNOWLEDGEMENTS

We thank Andrea Sekulovic and Marcin Lukasz Urbanowicz for their contributions to this study. Funding was provided by the Danish Research Council for technology and production sciences (FTP) grant no. 274-05-0017. Funding to pay the Open Access publication charges for the article was provided by FTP.

*Conflict of interest statement.* None declared.

## REFERENCES

- Heid, C.A., Stevens, J., Livak, K.J. and Williams, P.M. (1996) Real time quantitative PCR. *Genome Res.*, **6**, 986–994.
- Kostrikis, L.G., Tyagi, S., Mhlanga, M.M., Ho, D.D. and Kramer, F.R. (1998) Molecular beacons - spectral genotyping of human alleles. *Science*, **279**, 1228–1229.
- Nazarenko, I.A., Bhatnagar, S.K. and Hohman, R.J. (1997) A closed tube format for amplification and detection of DNA based on energy transfer. *Nucleic Acids Res.*, **25**, 2516–2521.
- Whitcombe, D., Theaker, J., Guy, S.P., Brown, T. and Little, S. (1999) Detection of PCR products using self-probing amplicons and fluorescence. *Nat. Biotechnol.*, **17**, 804–807.
- Isacson, J., Cao, H., Ohlsson, L., Nordgren, S., Svanvik, N., Westman, G., Kubista, M., Sjoback, R. and Sehlstedt, U. (2000) Rapid and specific detection of PCR products using light-up probes. *Mol. Cell. Probes*, **14**, 321–328.
- Higuchi, R., Dollinger, G., Walsh, P.S. and Griffith, R. (1992) Simultaneous amplification and detection of specific DNA-sequences. *Biotechnology*, **10**, 413–417.
- Higuchi, R., Fockler, C., Dollinger, G. and Watson, R. (1993) Kinetic PCR analysis - real-time monitoring of DNA amplification reactions. *Biotechnology*, **11**, 1026–1030.
- Wittwer, C.T., Herrmann, M.G., Moss, A.A. and Rasmussen, R.P. (1997) Continuous fluorescence monitoring of rapid cycle DNA amplification. *Biotechniques*, **22**, 130–138.
- Ririe, K.M., Rasmussen, R.P. and Wittwer, C.T. (1997) Product differentiation by analysis of DNA melting curves during the polymerase chain reaction. *Anal. Biochem.*, **245**, 154–160.
- Panicker, G., Myers, M.L. and Bej, A.K. (2004) Rapid detection of *Vibrio vulnificus* in shellfish and Gulf of Mexico water by real-time PCR. *Appl. Environ. Microbiol.*, **70**, 498–507.
- Woo, T.H.S., Patel, B.K.C., Cinco, M., Smythe, L.D., Symonds, M.L., Norris, M.A. and Dohnt, M.F. (1998) Real-time homogeneous assay of rapid cycle polymerase chain reaction product for identification of *Leptonema illini*. *Anal. Biochem.*, **259**, 112–117.
- Varga, A. and James, D. (2006) Real-time RT-PCR and SYBR Green I melting curve analysis for the identification of Plum pox virus strains C, EA, and W: effect of amplicon size, melt rate, and dye translocation. *J. Virol. Methods*, **132**, 146–153.
- Mori, S., Sugahara, K., Uemura, A., Akamatsu, N., Tutsumi, R., Kuroki, T., Hirakata, Y., Atogami, S., Hasegawa, H. et al. (2006) Rapid, simple, and accurate detection of K-ras mutations from body fluids using real-time PCR and DNA melting curve analysis. *Labmedicine*, **37**, 286–289.
- Myers, M.A. (1998) Direct measurement of cell numbers in microtitre plate cultures using the fluorescent dye SYBR green I. *J. Immunol. Methods*, **212**, 99–103.
- Jung, M., Muche, J.M., Lukowsky, A., Jung, K. and Loening, S.A. (2001) Dimethyl sulfoxide as additive in ready-to-use reaction mixtures for real-time polymerase chain reaction analysis with SYBR Green I dye. *Anal. Biochem.*, **289**, 292–295.
- Karsai, A., Muller, S., Platz, S. and Hauser, M.T. (2002) Evaluation of a homemade SYBR (R) Green I reaction mixture for real-time PCR quantification of gene expression. *Biotechniques*, **32**, 790–796.
- Nath, K., Sarosy, J.W., Hahn, J. and Di Como, C.J. (2000) Effects of ethidium bromide and SYBR (R) Green I on different polymerase chain reaction systems. *J. Biochem. Biophys. Methods*, **42**, 15–29.
- Giglio, S., Monis, P.T. and Saint, C.P. (2003) Demonstration of preferential binding of SYBR Green I to specific DNA fragments in real-time multiplex PCR. *Nucleic Acids Res.*, **32**, e106; p. 5.
- Xu, H.X., Kawamura, Y., Li, N., Zhao, L.C., Li, T.M., Li, Z.Y., Shu, S.N. and Ezaki, T. (2000) A rapid method for determining the G + C content of bacterial chromosomes by monitoring fluorescence intensity during DNA denaturation in a capillary tube. *Int. J. Syst. Evol. Microbiol.*, **50**, 1463–1469.
- Bengtsson, M., Karlsson, H.J., Westman, G. and Kubista, M. (2003) A new minor groove binding asymmetric cyanine reporter dye for real-time PCR. *Nucleic Acids Res.*, **31**, e45.
- Ishiguro, T., Saitoh, J., Yawata, H., Yamagishi, H., Iwasaki, S. and Mitoma, Y. (1995) Homogeneous quantitative assay of hepatitis-C virus-rna by polymerase chain-reaction in the presence of a fluorescent intercalator. *Anal. Biochem.*, **229**, 207–213.
- Wittwer, C.T., Reed, G.H., Gundry, C.N., Vandersteen, J.G. and Pryor, R.J. (2003) High-resolution genotyping by amplicon melting analysis using LCGreen. *Clin. Chem.*, **49**, 853–860.
- Monis, P.T., Giglio, S. and Saint, C.P. (2005) Comparison of SYTO9 and SYBR Green I for real-time polymerase chain reaction and investigation of the effect of dye concentration on amplification and DNA melting curve analysis. *Anal. Biochem.*, **340**, 24–34.
- Giglio, S., Monis, P.T. and Saint, C.P. (2005) *Legionella* confirmation using real-time PCR and SYTO9 is an alternative to current methodology. *Appl. Environ. Microbiol.*, **71**, 8944–8948.
- Machiels, B.M., Ruers, T., Lindhout, M., Hardy, K., Hlavaty, T., Bang, D.D., Somers, V., Baeten, C., von Meyenfeldt, M. and Thunnissen, F. (2000) New protocol for DNA extraction of stool. *Biotechniques*, **28**, 286–290.
- Bang, D., Pedersen, K. and Madsen, M. (2001) Development of a PCR assay suitable for *Campylobacter* spp. mass screening programs in broiler production. *J. Rapid Methods Autom. Microbiol.*, **9**, 97–113.
- Keramas, G., Bang, D.D., Lund, M., Madsen, M., Rasmussen, S.E., Bunkenborg, H., Telleman, P. and Christensen, C.B.V. (2003) Development of a sensitive DNA microarray suitable for rapid detection of *Campylobacter* spp. *Mol. Cell. Probes*, **17**, 187–196.
- Zipper, H., Brunner, H., Bernhagen, J. and Vitzthum, F. (2004) Investigations on DNA intercalation and surface binding by SYBR Green I, its structure determination and methodological implications. *Nucleic Acids Res.*, **32**, e103; p. 10.
- Wu, P., Li, H., Nordlund, T.M. and Rigler, R. (1990) Multistate modeling of the time and temperature dependence of fluorescence from 2-aminopurine in a DNA decamer. *Time-Resolved Laser Spectroscopy in Biochemistry II*, **1204**, 262–269.
- Chen, R.F. and Knutson, J.R. (1988) Mechanism of fluorescence concentration quenching of carboxyfluorescein in liposomes - energy-transfer to nonfluorescent dimers. *Anal. Biochem.*, **172**, 61–77.
- Herrmann, M.G., Durtschi, J.D., Bromley, L.K., Wittwer, C.T. and Voelkerding, K.V. (2006) Amplicon DNA melting analysis for mutation scanning and genotyping: cross-platform comparison of instruments and dyes. *Clin. Chem.*, **52**, 494–503.
- Lin, Y.W., Chiu, T.C. and Chang, H.T. (2003) Laser-induced fluorescence technique for DNA and proteins separated by capillary electrophoresis. *J. Chromatogr. B Analyt. Technol. Biomed. Life Sci.*, **793**, 37–48.
- Yan, X.M., Grace, W.K., Yoshida, T.M., Habbersett, R.C., Velappan, N., Jett, J.H., Keller, R.A. and Marrone, B.L. (1999) Characteristics of different nucleic acid staining dyes for DNA fragment sizing by flow cytometry. *Anal. Chem.*, **71**, 5470–5480.
- Petty, J.T., Bordelon, J.A. and Robertson, M.E. (2000) Thermodynamic characterization of the association of cyanine dyes with DNA. *J. Phys. Chem. B*, **104**, 7221–7227.
- Yan, X.M., Hang, W., Majidi, V., Marrone, B.L. and Yoshida, T.M. (2002) Evaluation of different nucleic acid stains for sensitive double-stranded DNA analysis with capillary electrophoretic separation. *J. Chromatogr. A*, **943**, 275–285.